





PEGylated Albumin-Based Drug Carriers for the Treatment of Experimental Stroke

Nazeli Zaqaryan¹, Rita Khallouf^{1,2}, Arpi Manukyan¹ , Vahe Atoyan¹, Astghik Tsokolakyan³ , Mkrtich A. Yeranossyan³ , Samvel G. Chailyan¹  and Kristine E. Danielyan^{1,2,*} 

¹Department of H. Buniatian Inst. of Biochem., National Academy of Sciences of the Republic of Armenia (NAS RA), Yerevan 0014, Armenia

²Department of Pharmacy, Eurasia Int. Univ., Yerevan 0014, Armenia

³Department of A. B. Nalbandyan Inst. of Chemical-Physics, National Academy of Sciences of the Republic of Armenia (NAS RA), Yerevan 0014, Armenia

Abstract:

Background: Stroke is the leading cause of mortality and disability worldwide. The goal of this study was to design stable, small-sized polyethylene glycol (PEG)/albumin nanoparticles (NPs) for delivering drugs targeting various phases of stroke recovery.

Methods: RP-HPLC (Reversed-Phase High-Performance Liquid Chromatography) and spectrophotometry were used to assess the stability and effectiveness of the drug carriers. The dynamic light scattering (DLS) technique was employed to evaluate the size and zeta potential of the particles. The integrity of the blood-brain barrier (BBB) in laboratory rats was assessed by measuring Evans Blue (EB) leakage after intracranial injection of 3% H₂O₂. AutoDock Tools 1.5.7 was used to analyze the compatibility of the polymers with albumin.

Results: The particles exhibited high drug-loading efficiency. In all groups, the most prevalent particle size averaged 211.09 ± 92.72 nm. The drug-loaded particles exhibited prolonged circulation and had a half-life (T_{1/2}) ranging from 7.64 to 13 days. Furthermore, both albumin particles and PEGylated albumin carriers loaded with dexamethasone and allopurinol significantly preserved blood-brain barrier (BBB) integrity (2.92 ± 0.4 µg, *p* < 0.04), as indicated by reduced Evans Blue (EB) extravasation (6.73 ± 0.58 µg) compared to the control group (9.12 ± 1.2 µg, *p* < 0.04, *t*-test).

Discussion: The protective effect of albumin carriers on the BBB may be attributed to an increase in blood oncotic pressure, which helps limit edema formation. PEG/albumin drug-loaded carriers demonstrated greater stability, as indicated by their zeta potential, and exhibited a more pronounced BBB-preserving effect due to the combined actions of albumin and the loaded drugs.

Conclusion: In this study, stable, layered NPs carrying different drugs were synthesized that could be applied for the treatment of experimental stroke.

Keywords: Carriers, Drugs, Dexamethasone, Allopurinol, Stability, Size, Oxidative brain damage.

© 2025 The Author(s). Published by Bentham Open.

This is an open access article distributed under the terms of the Creative Commons Attribution 4.0 International Public License (CC-BY 4.0), a copy of which is available at: <https://creativecommons.org/licenses/by/4.0/legalcode>. This license permits unrestricted use, distribution, and reproduction in any medium, provided the original author and source are credited.

*Address correspondence to this author at the Department of H. Buniatian Inst. of Biochem., National Academy of Sciences of the Republic of Armenia (NAS RA), Yerevan 0014, Armenia and Department of Pharmacy, Eurasia Int. Univ., Yerevan 0014, Armenia; E-mail: kristine_danielyan@biochem.sci.am

Cite as: Zaqaryan N, Khallouf R, Manukyan A, Atoyan V, Tsokolakyan A, Yeranossyan M, Chailyan S, Danielyan K. PEGylated Albumin-Based Drug Carriers for the Treatment of Experimental Stroke. Open Biotechnol J, 2025; 19: e18740707379038. <http://dx.doi.org/10.2174/0118740707379038250617195726>



CrossMark

Received: January 05, 2025

Revised: April 02, 2025

Accepted: May 13, 2025

Published: July 14, 2025



Send Orders for Reprints to
reprints@benthamscience.net

1. INTRODUCTION

Stroke is ranked as the top cause of death and stands as the major contributor to disability worldwide [1, 2]. Despite advances in the field of the treatment of acute stroke, the development of new interventions remains necessary, and the clinical translation of these interventions is slow. Several factors contribute to this delay in improvements, including the limited therapeutic time window for drugs (such as tissue-type plasminogen activator and its derivatives, such as alteplase, reteplase, and tenecteplase), patient heterogeneity, reliance on suboptimal animal models, and challenges related to drug safety and pharmacokinetics [3-5].

Long-term treatment includes medications to prevent recurrence (such as antiplatelets, anticoagulants, *etc.*) and to facilitate rehabilitation (physical, occupational, and speech therapy). Advanced therapies can target inflammation and oxidative stress to protect brain cells and enhance recovery. Another aspect of the treatment is managing risk factors, such as high blood pressure, cholesterol, and diabetes [6].

Nanoparticle (NP)-based drug delivery systems (DDS) offer significant improvements in drug pharmacokinetics, pharmacodynamics, and safety by protecting drugs from early deactivation and clearance, providing targeted access to specific sites, and preventing off-target interactions.

These technical improvements result in prolonged circulation time, increased drug accumulation in targeted regions, and reduced dosage requirements, which certainly minimizes toxicity [7]. The behavior of a nanoparticle (NP) carrier is determined by several important factors. Firstly, size plays a vital role, influencing biodistribution, cellular internalization, and clearance by immune cells and the reticuloendothelial system (RES). Particles with diameters smaller than 200 nm are generally preferred because smaller carriers may experience low encapsulation efficiency and rapid drug release, while larger particles can potentially cause the formation of clots in the microvasculature. Secondly, shape determines transporting properties, cellular uptake, stability, and the available surface area for functionalization and interactions with the surrounding environment. Thirdly, rigidity is a significant factor; flexible or deformable carriers demonstrate improved uptake and efficient tissue penetration [7].

Additionally, hydrophobicity and surface charge are crucial, as they impact carrier toxicity, tendency for aggregation, interactions with cell membranes, and adsorption by serum proteins. The mechanisms of particle degradation and drug release are equally important because these phenomena control the precise unloading of the encapsulated drug while maintaining stability at the site of action [8].

One class of nanoparticles that has garnered significant attention is PEGylated NPs, which are coated with polyethylene glycol (PEG). These particles are known for their ability to improve drug stability and bioavailability, particularly in challenging conditions like cancer and stroke. PEGylated NPs have demonstrated success in various applications. For example, it has been found that when incorporated into PEGylated nanotubes, the anticancer medi-

cation doxorubicin reduced the size of tumors in mice [9]. When doxorubicin-loaded PEG-nanotubes were injected intratumorally and, to a lesser extent, intravenously, tumor size was found to be reduced *in vivo* even more extensively [9]. Nucleic acid-functional nanoparticles have been demonstrated to be effectively delivered to a variety of cancer cells using PEGylated mesoporous silica and polysilsesquioxane nanoparticles [10, 11].

Beyond cancer, PEGylated lipid nanoparticles have been instrumental in mRNA vaccine delivery. Pfizer/BioNTech and Moderna vaccines are two lipid-based formulations that include PEG and methoxy-PEG, respectively, and are approved for emergency use in the US and numerous other countries [12]. They transmit mRNA encoding the SARS-CoV-2 antigen [13].

Numerous data exist regarding the application of PEGylated nanoparticles in the setting of experimental stroke. PEGylated NPs have gained popularity recently because of their high blood-brain barrier (BBB) permeability. A single intravenous injection of PEG with curcumin (30% wt/wt) not only targets the central nervous system at the site of injury but also reduces the apparent diffusion coefficient, which is linked to cytotoxic edema in the brain [14]. This indicates that substances that are often unable to cross the BBB may be able to do so after binding with PEG. Recent research using curcumin has shown that, after brain ischemia-reperfusion in rats, the applied formulation with PEG and polylactide-co-glycolide (PLGA) was more effective than curcumin alone at lowering reactive oxygen species and apoptosis [14]. Due to the poor biodistribution of free curcumin to the brain, higher doses are required to achieve comparable therapeutic efficacy [14].

Interestingly, another group created a novel formulation of isoliquiritigenin (ISL)-loaded micelles, which were prepared with DSPE-PEG2000 as the drug carrier and modified with the brain-targeting polypeptide angiopep-2. Such a strategy enhanced the physicochemical properties of the particles, transforming them into well-water-soluble carriers with high bioavailability of ISL for the treatment of acute ischemic stroke [15].

The extent of the data related to the targeting of ischemic stroke with liposomes loaded with a statin is insufficient. A group of investigators studied the impact of atorvastatin-loaded PEG (polyethylene glycol) conjugated liposomes (LipoStatin) on outcomes in rats with cerebral ischemia-reperfusion [16]. The researchers modeled PEGylated liposomes loaded with atorvastatin in a way that these nanoparticles would specifically target and accumulate in the ischemic region to ameliorate the harmful effects of the stroke [16].

Based on the existing results, PEG is able to enhance the pharmacokinetics of drugs, particularly those with a protein-like nature. Albumin is one of the known carriers of medications, with limited encapsulation abilities and a short circulation time in the bloodstream.

The aim of this work was to create layered albumin/PEG particles efficiently loaded with drugs for the treatment of different stages of stroke. The NPs were composed of additional compounds, each with specific therapeutic effects:

albumin, which increases blood oncotic pressure and aids in reducing brain edema following stroke [17]; dexamethasone, which alleviates post-stroke inflammation; and allopurinol, which inhibits xanthine oxidoreductase activity (XOR; EC: 1.17.3.2) [18].

The particles were also characterized based on physico-chemical properties, and their stability was evaluated. The stabilizing effect of PEG was compared with that of other biological as well as chemical polymers using *in situ* analyses. This study examined the circulation properties of the particles and characterized the pharmacokinetics of the new formulations.

Finally, the impact of the prepared particles was evaluated in the setting of experimental oxidative brain damage. Oxidative brain damage caused by excessive free radical formation after cerebral vessel injury is a critical stage in stroke development, and was a central focus of our current work.

2. MATERIALS AND METHODS

All reagents were purchased from Sigma-Aldrich-Merck. The human serum albumin (HSA) 10% was purchased from Arpimed (Armenia). Glutaraldehyde 40% (GA) was purchased from Medisar (Armenia).

2.1. Molecular Docking

The structure of the HSA (PDB ID: 1AO6) used in this study was obtained from the Worldwide Protein Data Bank [19]. The 2D chemical structures of the following compounds were obtained from the PubChem database [20]: butyric acid (PubChem CID = 264), ethylene glycol (PubChem CID = 174), lactic acid (PubChem CID = 612), lysine (PubChem CID = 5962), cholesterol (PubChem CID = 5997), inositol (PubChem CID = 892), ethanolamine (PubChem CID = 700), choline (PubChem CID = 305), vinyl acetate (PubChem CID = 7904), and ethylenimine (aziridine) (PubChem CID = 9033).

The 3D structures of the chemical compounds were obtained using Open Babel [21, 22]. Preparation of the basic source files for molecular docking, which included the determination of grid box coordinates and format conversion, was performed using AutoDock [22, 23]. Molecular docking was performed using AutoDockTools 1.5.7 with all default settings, except for the exhaustiveness parameter, which was set to 128 for enhanced reliability. AutoDockTools 1.5.7, PyMol, and BIOVIA Discovery Studio visualizer programs were used for the generation and analysis of the results [22].

2.2. Generation of the Albumin Particles

Five hundred microliters of 10% bovine albumin (Arpimed, Armenia) was dissolved in 1 ml of water [24]. Ten microliters of GA (40%) was added along with 1 ml of lithium. After this, the mixture was incubated for 24 hours. The mixture was centrifuged at 14,000 RPM for 30 minutes. The precipitate was dissolved in 1 ml of water. The particles were washed to remove the remaining GA by dialysis against 0.1 M phosphate-buffered saline (PBS) (pH ~ 7.4) [24, 25]. Additionally, for the formation of the shell of the albumin particles, we used 10% PEG 2000, 3000, 12000,

and 32000. The concentration of dexamethasone used was 4 mg/mL. Allopurinol was used at 0.007%. After preparing the particles, the suspensions for each group were dialyzed for 24 hours to remove the small reagents used in the polymerization process.

2.3. Fluorescence Confocal Microscopy

An inverted microscope (Model: Leica DM8) was used for imaging the particles. The microscope was equipped with traditional transmitted light, a fluorescence system, three laser lines (488 nm, 532 nm, and 635 nm), and a tunable emission detector. The system was equipped with LAS X software to process the acquired images. All particles were labeled with albumin-specific Evans Blue dye before imaging.

2.4. Measurement of the Zeta Potential of the Particles

The hydrodynamic diameters of the particles were measured using the dynamic light scattering method with a Litesizer™ 500 (Anton Paar, Graz, Austria). Measurements were conducted under automatic settings optimized for latex spheres at 25°C. The ζ -potential was measured using an Omega cuvette Z (Anton Paar) with a 40 mW laser and a wavelength of 658 nm. Each analysis was performed over 40 runs to ensure accuracy [24].

2.5. Reverse-phase HPLC

The detection of dexamethasone and allopurinol was performed using reverse-phase HPLC on a Shimadzu LC-20 chromatograph (Shimadzu, Kyoto, Japan) equipped with a UV-Vis detector SM 5000 and C18 RP columns produced by Avex (Tokyo, Japan), Waters (MA, USA), and Symmetry (AZ, USA). Elution was performed at a flow rate of 0.6 mL/min under isocratic conditions using a 70:30 (v/v) acetonitrile: water ratio. Allopurinol was detected at 260 nm, whereas dexamethasone was detected at 242 nm [24].

2.6. Vertebrate Animals

Experiments involving animals were conducted in compliance with IACUC policies, by the US National Research Council's "Guide for the Care and Use of Laboratory Animals" and animal care standards, as well as the regulations established by the Armenian Ethical Committee of the Institute of Biochemistry named after H. Buniatian, National Academy of Sciences of the Republic of Armenia (International Registration N IRB0001621; IORG 0009782; Reference Letter (Approval N) 7, 2024). Accepted international procedures, including anesthesia, euthanasia, animal surgery, and blood collection, were performed based on the regulations, policies, and guidelines written and approved by the organizations mentioned above.

Healthy white laboratory male rats, 8–9 months old (weight = 200 g; n = 41), were anesthetized via intraperitoneal injection of pentobarbital at a dose of 2 mg per 100 g of body weight, based on symptomatic and genetic verification by the veterinarian. The animals were purchased from the L.A. Orbeli Institute of Physiology, National Academy of Sciences of Armenia. The specified dosage typically induced anesthesia within 5 minutes. The depth of anesthesia was evaluated by gently squeezing the animals'

legs with forceps; a lack of response indicated adequate anesthesia. When necessary, additional doses were administered to maintain proper anesthesia depth.

To support the animals' normal physiological state during surgery, cranial and rectal temperatures were continuously monitored. After seven days, the animals were deeply anesthetized and euthanized through cervical dislocation. Entire pre-surgical, surgical, and post-surgical observations were carefully documented [24, 25].

Two types of animal experiments were performed: 1. circulation experiments, and 2. experiments related to the evaluation of the integrity of the BBB after intracranial injection of hydrogen peroxide (3%). For each experimental group, 3–5 animals were used. Based on our experience, the mentioned sample size was sufficient for obtaining accurate results [26–28], due to the fluorescence as well as high absorbance abilities of Evans Blue used in both types of the above-mentioned experiments.

The circulation set of experiments included the following animal groups injected with a. albumin particles (control), b. albumin particles coated with PEG, c. PEG/albumin particles coated with drugs, and d. PEG/albumin particles loaded with medicines. There were no inclusion or exclusion criteria for the animals in the experiments.

The second set of experiments was devoted to evaluating the possible protective abilities of a. albumin particles (control), b. albumin particles coated with PEG, c. PEG/albumin particles covered with drugs, and d. PEG/albumin particles loaded with medicines under conditions of experimental brain oxidative damage, reflecting one of the stages of experimental stroke development. Animals were injected with the formulations if they survived the surgery and were included in the experimental group only if anesthesia did not last more than 40 minutes.

All animals were kept under similar conditions. The experiments were conducted in a blinded manner by separate research groups.

2.7. Circulation of Particles

The animals were injected with $1.08\text{--}1.10 \times 10^8$ albumin particles *via* the jugular vein. Blood samples were collected at various time points into heparin-coated vacutainers. The elimination constant, K_{el} , was calculated using Eq. (1) [29, 30]. The half-life $T_{1/2}$ was evaluated using Eq. (2) [29, 30], as outlined in previous studies [24]. The equations are as follows:

$$K_{el} = \text{Slope} \times (-0.23) \quad (1)$$

$$T_{1/2} = 0.64/K_{el} \quad (2)$$

The blood samples were centrifuged at 1000 RPM for 10 minutes, and the plasma containing the particles was separated. The number of particles in the plasma was calculated using a hemocytometer. Images were captured, and particle counts were quantified using Pixcavator 5 software (Pixcavator Software, developed by Peter Saveliev, Marshall University, WV, USA). A trinocular phase-contrast microscope (Boeco GmbH), equipped with a 100× objective, was utilized for visualization and calculation of the number of particles [24].

2.8. Modeling of Brain Damage in Rats

First, a small craniotomy was performed. Five microliters of 3% hydrogen peroxide was injected into the brain parenchyma of the animals using the following coordinates relative to the bregma: 2 mm lateral to the midline, 4 mm anterior to the coronal suture, and 3 mm below the skull surface. Prior to the procedure, the rats were fixed in a stereotaxic frame. A syringe connected to a 27-gauge stainless steel cannula with a 30° bevel was carefully inserted into the brain parenchyma. After the infusion, the cannula was left in place for 2 minutes to ensure proper delivery and was then slowly withdrawn. The burr hole was sealed with bone wax, the scalp incision was sutured, and the animals were returned to their cages with unrestricted access to food and water [26, 27].

2.9. Evans Blue Extraction from the Brain Tissue

The integrity of the blood-brain barrier (BBB) was evaluated by measuring the amount of Evans Blue (EB) dye (4% in saline, 4 mL/kg, injected intravenously *via* the femoral vein two hours before sacrifice) that penetrated the brain parenchyma. The procedure for EB extraction was as follows: under anesthesia, the chest was opened, and saline perfusion was performed through the left ventricle until the perfusion fluid flowing out from the right atrium appeared colorless [26]. After decapitation, the brain was sliced into two parts at the levels of bregma +2.7 mm and −0.3 mm. Coronal blocks were further divided into the right and left hemispheres, and regions of interest were isolated for local EB dye measurement [26].

The brain tissue was homogenized and centrifuged, and the dye was extracted using ethanol (at a 1:3 ratio). The concentration of EB was determined using a spectrophotometer at 620 nm (Cary 60, Agilent, USA). The dye content in the tissue was calculated using external standards prepared in the same solvent (100–500 ng/mL). The tissue EB levels were quantified from a linear standard curve generated from known dye concentrations and expressed as absolute values [26, 27].

2.10. Statistical Analysis of the Results

Data are presented in the work as mean ± SEM. Statistical significance between control and experimental groups was calculated using one-way analysis of variance (ANOVA) or the Student t-test (SigmaStat 10, Excel). Before applying the ANOVA test, SigmaStat 10 automatically ran a normality test to verify the distribution of the means of the groups' samples.

The statistical power was set at 80% for the calculation of significance between the experimental groups and the control, with a significance level of $p < 0.05$. The number of variables per group, calculated by the SigmaStat program, was also taken into consideration.

3. RESULTS AND DISCUSSION

3.1. Docking Analyses of the Polymers Used for the Preparation of Drug Carriers

Polymers of chemical or biological origin can be applied for the generation of particles used for drug delivery.

A cholesterol-rich nano-emulsion (LDE) can serve as a transporting agent for chemotherapeutic drugs in the bloodstream and target them to neoplastic and inflammatory tissues. This approach enhances the drug's biodistribution and reduces systemic toxicity [31].

Choline might serve as an ionic coating material for the delivery of drugs into the brain parenchyma [32]. To enable distribution while minimizing coprecipitation and functionalization of ferrite NPs, ethanolamine (EA), along with other compounds, may be effectively used [33].

Sugar alcohols are phase-change materials with several benefits, but they may experience leakage during use. Mo S. and Li Y. *et al.* synthesized inositol nano-capsules under different conditions, varying the number of precursors and the timing of their addition [34].

Another monomer is vinyl acetate, which might serve as a component of polyvinyl alcohol (PVA) nanoparticles. These particles can be synthesized using the water-in-oil emulsion technique, with PVA acting as a stabilizer to regulate particle size and morphology. Due to its hydrophilic nature and compact structure, PVA is often used in conjunction with other polymers and nanomaterials to enhance the composite's barrier properties [35].

Messenger RNA (mRNA) vaccines have been widely used worldwide to fight the COVID-19 pandemic. These vaccines consist of non-amplifying mRNA encapsulated in lipid nanoparticles (LNPs), which have become the benchmark for non-viral nucleic acid delivery carriers. However, the formulation and production of these mRNA-LNP nanoparticles are expensive and time-consuming.

To overcome these challenges, researchers have employed self-amplifying mRNA (saRNA) and developed novel polymers as alternative non-viral carriers to LNPs. This innovative approach has enabled the simple and rapid one-pot formulation of saRNA-polyplexes. The polymer-based carrier scaffold consisted of ethylenimine and propylenimine comonomers, resulting in linear poly(ethylenimine-ran-propylenimine) (L-PEIx-ran-PPIy) copolymers with precisely controllable degrees of polymerization [36].

Butyric acid has been shown to enhance the radiosensitivity of cancer cell lines *in vitro*; however, its short systemic half-life has limited its effectiveness *in vivo*. To overcome the unfavorable pharmacokinetics of low-molecular-weight (LMW) butyric acid, N. Madbouly, A. Ooda, and colleagues created a novel polymeric prodrug using amphiphilic block copolymers, specifically poly (ethylene glycol)-b-poly(vinyl butyrate) (PEG-b-PV(BA)).

This prodrug incorporates multiple butyric acid units conjugated through enzymatically degradable ester linkages within the hydrophobic segment. The PEG-b-PV(BA) copolymers spontaneously self-assemble into nanoparticles (NanoBA) with diameters in the nanometer range [37, 38].

Poly(D,L-lactic acid) (PLA) is widely used in the biomedical field due to its biodegradable, biocompatible, and non-toxic properties. Numerous techniques, including emulsion, salting out, and precipitation, have been employed to optimize PLA micro- and nanoparticle formulations. These particles serve as controlled drug delivery systems for therapeutic agents, including proteins, genes, vaccines, and medications.

Particles made from PLA mostly have low loading capacity, limited encapsulation efficiency, and difficulties with terminal sterilization. However, the utility of these NP materials remains an important, clinically viable solution [39, 40].

Poly(amino acids) are effective as drug carriers for delivering anticancer drugs. Studies have focused on confirming the role of isomers in the formation of nanoparticles. Yu, B., and Lang, X. demonstrated in their study that two polylysine isomers, ϵ -polylysine (ϵ -PL) and α -polylysine (α -PL), exhibit different capacities for entrapping methotrexate (MTX) and functioning as nano-drug delivery systems [41].

First, we conducted docking analyses to compare the affinity of ethylene glycol, the monomer of PEG, with that of other possible monomers, focusing on their interaction with the main component of the carriers, *i.e.*, albumin (Fig. 1A-D). Ethylene glycol interacted with albumin through the formation of a conventional hydrogen bond involving LEU 516. It also showed an unfavorable donor-donor interaction with ARG 521 and a van der Waals interaction with GLU 167.

To compare the effectiveness of different monomers with that of PEG, we selected seven compounds, which are presented below.

Butyric acid interacted with albumin through a hydrogen bond between the oxygen atom of the acid molecule and ARG 410 of albumin. An alkyl-alkyl interaction was also observed.

Lactic acid formed an unfavorable acceptor-acceptor interaction with TYR 150 and hydrogen bonds with ARG 257 and SER 287.

Lysine formed five conventional hydrogen bonds between its two negatively charged carboxyl oxygens, the hydrogens of its amino groups, and the nitrogen of one amino group with the following residues of albumin: LYS 195, GLU 153, SER 192, TYR 150, and ARG 257. Additionally, LYS 199 and TYR 150 were involved in alkyl-type interactions.

Cholesterol, due to the formation of multiple alkyl-type interactions, interacted with albumin (Fig. 2A).

Inositol was able to bind to albumin through hydrogen bond formation with SER 192 and ARG 257, and an unfavorable donor-donor interaction with HIS 288 was observed (Fig. 2B).

The hydrogen of the hydroxyl group of ethanolamine formed a hydrogen bond with SER 192 of albumin (Fig. 2C).

Similarly, the hydrogen of the hydroxyl group of choline formed a hydrogen bond with TYR 161 of albumin (Fig. 2D).

A highly negatively charged oxygen atom of vinyl acetate formed a hydrogen bond with ARG 257 of albumin (Fig. 2E).

Ethylenimine interacted with GLU 153 of albumin through a hydrogen bond involving the hydrogen atom connected to its nitrogen atom (Fig. 2F).

Interestingly, PEG, which is widely accepted as one of the best drug carriers due to its biodegradability, exhibited one of the lowest affinities and binding energies toward albumin compared to the other monomers analyzed in this study (Table 1).

As mentioned in Table 1, cholesterol, due to its steroid ring structure, which is very similar to that of the reference compound dexamethasone, exhibited the highest binding affinity and the most negative binding energy value. Positively charged compounds, through the formation of hydrogen bonds with albumin, also demonstrated high binding affinity values. Examples include lysine and choline.

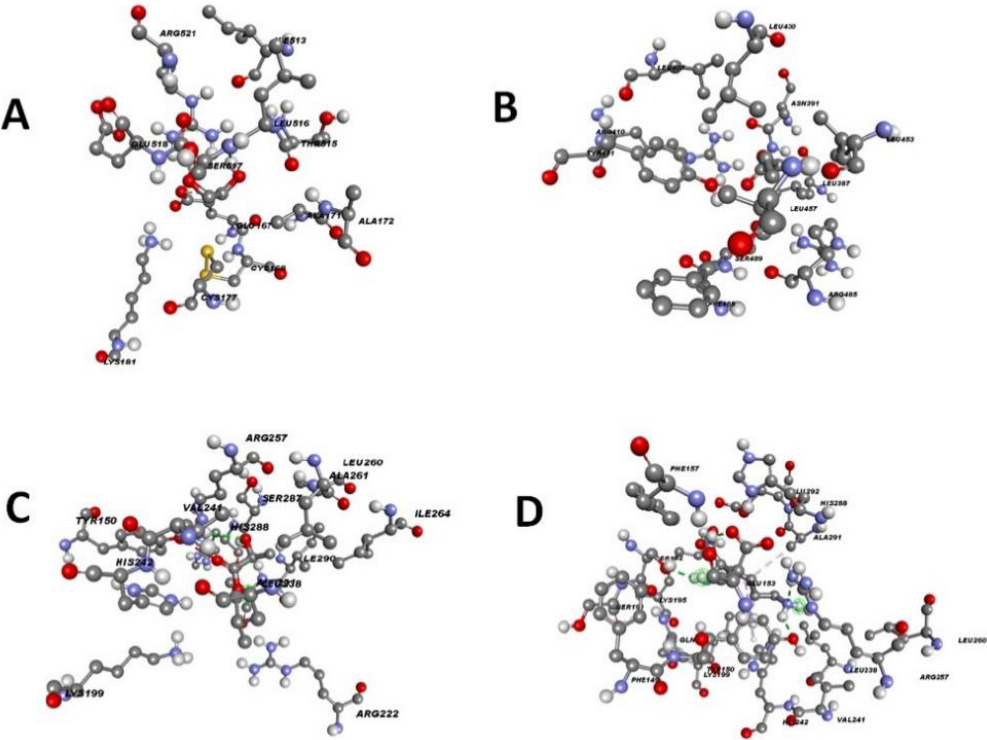


Fig. (1). Interaction between albumin and ethylene glycol, butyric acid, lactic acid, and lysine. **A.** Interaction of the albumin with the ethylene glycol (ID =174). **B.** Interaction of the albumin with the butyric acid (ID =264). **C.** Interaction of the albumin with the lactic acid (ID =612). **D.** Interaction of the albumin with the lysine (ID =5962).

Table 1. Comparison of the effectiveness of the binding of monomers to the molecule of albumin

Compounds	Binding Affinity (Kcal/mol)	Binding Energy (kcal/mol)	RMSD
Cholesterol	-8.58	-5.30	35.497
Ethanolamine	-2.65	-2.92	37.761
Choline	-3.2	-2.40	39.881
Inositol	-5.3	-1.77	38.279
Vinyl Acetate	-3.56	-2.29	40.14
Ethylenimine	-2.07	-2.60	30.936
Butyric acid	-3.8	-2.76	37.539
Ethylene Glycol	-2.9	-1.86	33.077
Lactic acid	-3.76	-2.58	35.2925
Lysine	-4.47	-2.23	36.131
Reference	-8.58	-4.10	37.318

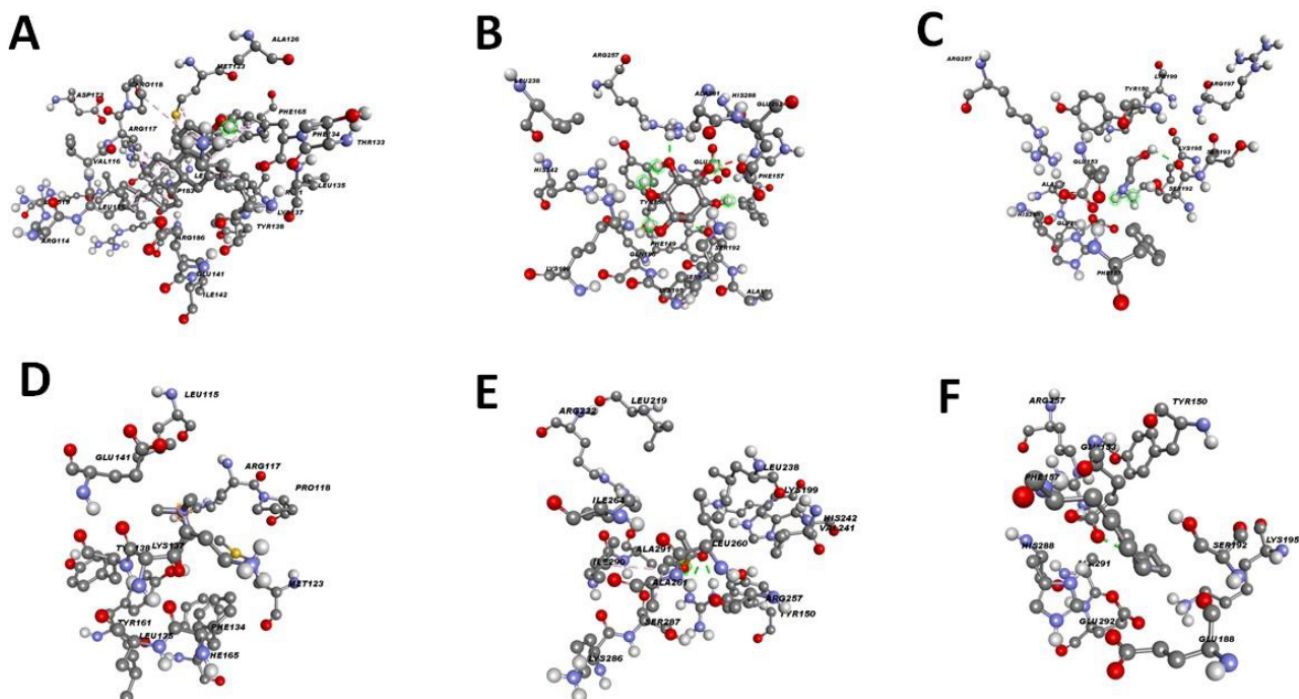


Fig. (2). Interaction between albumin and various monomers used in the generation of drug carriers. A. Interaction of the albumin with the cholesterol (ID = 5997), B. Interaction of the albumin with the inositol (ID = 892), C. Interaction of the albumin with the ethanolamine (ID = 700), D. Interaction of the albumin with the choline (ID = 305), E. Interaction of the albumin with the vinyl acetate (ID = 7904), and F. Interaction of the albumin with the ethylenimine (ID = 9033).

The acids, vinyl acetate, butyric acid, and lactic acid, due to their negative charges and ability to form hydrogen bonds, exhibited similar binding affinities, such as -3.56 kcal/mol, -3.8 kcal/mol, and -3.76 kcal/mol, respectively.

Inositol, a small molecule with six hydroxyl groups, readily formed hydrogen bonds with atoms of albumin, resulting in a high binding affinity of -5.3 kcal/mol.

Ethanolamine, a small, highly polarized molecule with high mobility and a hydroxyl group, also formed hydrogen bonds with albumin.

The lowest binding affinity among the monomers listed in Table 1 belonged to ethylenimine (-2.07 kcal/mol), which primarily serves as an auxiliary reagent in particle formation, rather than as a main structural component.

3.2. Efficiency of Drug Encapsulation and/or Attachment to the Carrier Particles

RP-HPLC was used to evaluate the entrapment and/or binding efficiency of drugs to PEG/albumin particles. Fig. (3A-G) illustrate the workflow of the analysis. Fig. (3A and B) show the peaks corresponding to the initially added amounts of allopurinol and dexamethasone, respectively.

Fig. (3C and D) show the amounts of dexamethasone and allopurinol that remained untrapped in the supernatant, allowing comparison with Fig. (3A and B). The bound percentages of the drugs were $94.16 \pm 0.5\%$ for

dexamethasone and $98.58 \pm 0.7\%$ for allopurinol.

Fig. (3E, F, H) present the unbound amounts of dexamethasone and allopurinol in formulations where the carriers were pre-shelled with the drugs. In these cases, the drug binding percentages were $89.61 \pm 0.8\%$ for dexamethasone and $87.0 \pm 0.48\%$ for allopurinol.

Overall, the results demonstrated that the incorporation of both drugs into the particle structures was extremely efficient.

3.3. Delineation of the Particle Size as well as the Zeta Potential

The majority of nanoparticles (NPs) with medicinal significance are designed to range in size from a few nanometers up to approximately 300 nm [42]. This size range facilitates intracellular uptake, resulting in a high surface-area-to-volume ratio that enhances the chemical reactivity and drug-loading capacity of the NPs. Further functionalization of the NP surface by adding targeting ligands provides opportunities for the development of highly selective nanomedical therapies targeting specific tissues or cell types.

Fig. (4A) illustrates the increase in particle size depending on the molecular weight of the PEG used. For PEG2000, the particle size was 263.47 ± 66.03 nm; for PEG3000, it was 764.49 ± 261.9 nm; for PEG12000, it was 3485.08 ± 1963.85 nm; and for PEG32000, it was 5299.21 ± 3076.83 nm.

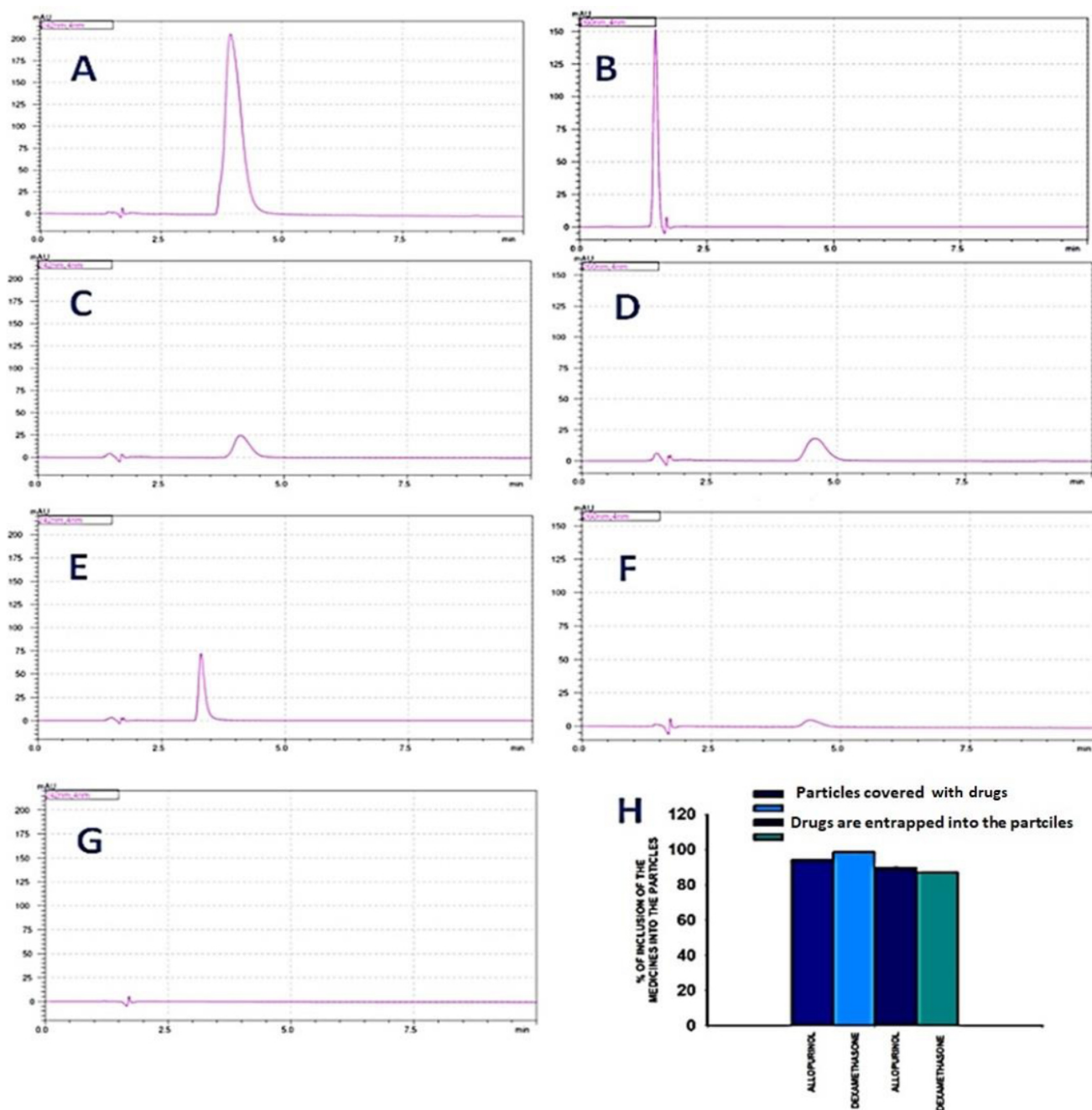


Fig. (3). Efficiency of allopurinol and dexamethasone entrapment and/or binding to PEG/albumin particles evaluated by RP-HPLC. The chromatography conditions were as follows: an isocratic regime, with a concentration of the eluent of 70% water and 30% acetonitrile. The speed of the elution was equal to 0.6 ml/min. The experiments used a C18 RP column. For each group, we had $n = 5$ samples. The representative chromatograms are included in the work. **A.** The absolute amount of dexamethasone used for the preparation of the carriers. **B.** Absolute amount of the allopurinol used for the preparation of the particles. **C.** The chromatogram represents the amount of unbound dexamethasone that remained in the solution after the formation of the carriers covered with the drugs. **D.** The chromatogram represents the amount of the unbound allopurinol that remained in the solution after the formation of the carriers covered with the drugs. **E.** The chromatogram represents the amount of unbound dexamethasone that remained in the solution after the formation of the carriers, which were entrapped with the drugs. **F.** The chromatogram represents the amount of unbound allopurinol that remained in the solution after the formation of the carriers, which were entrapped with the drugs. **G.** The background chromatogram. **H.** Calculation of the absolute bound amount of allopurinol and dexamethasone based on the linearity of the dependence of the concentration of the drugs on the area of the peaks.

Based on previously developed methods, we prepared albumin nanoparticles with two major size populations: one with an average diameter of 22.65 nm, representing 72.9% of the sample, and the second with an average diameter of 421.05 nm, representing 27.1% (Fig. 4B). After filtration, the PEG/albumin particles exhibited two size populations as well: 164.1 nm, comprising 98.89% of the particles, and 3119.61 nm, comprising 1.11% (Fig. 4C).

The diameter of the drug-loaded particles was distributed across three populations: 7.1 nm (13.8%), 217.16 nm

(27.9%), and 554.5 nm (58.26%) (Fig. 4D). In the case of albumin/PEG particles coated with drug, the size distribution also revealed three primary populations: 8.64 nm (69.4%), 55.9 nm (18.62%), and 255.7 nm (11.94%) (Fig. 4E).

We also characterized the zeta potential, as a measure of the stability, of the particles. For albumin, it was 13.69 ± 0.74 mV, for PEG/albumin particles, it was 18.99 ± 1.4 mV, for PEG/albumin particles loaded with the drugs, it was 14.88 ± 2.063 mV, and for albumin/PEG carriers covered with the drugs, it was 15.23 ± 1.53 mV (SEM).

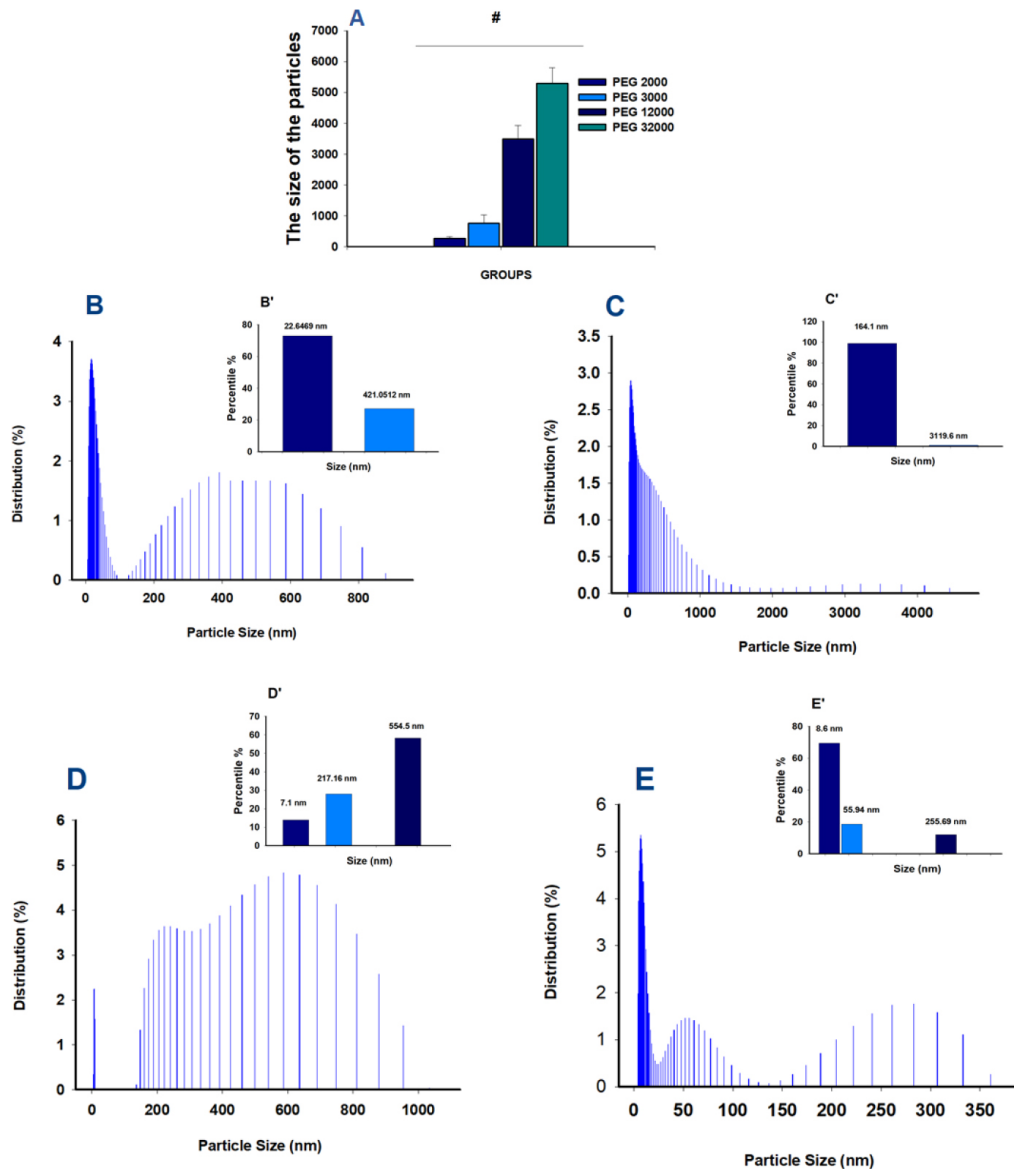


Fig. (4). Evaluation of the size of the generated drug carriers. The number of measurements for every group was equal to 6. **A**. Dependence of the particle's size on the PEG's Molecular Weight (MW). **B**. Percentile of the distribution of albumin particles. **B'**. Insert: Percentile of NPs distribution in the albumin group **C**. Percentile of the distribution of PEG/albumin particles. **C'**. Insert: Percentile of NPs distribution in PEG/albumin group. **D**. Percentile of the distribution of PEG/albumin particles loaded with the drug's particles. **D'**. Insert: Percentile of NPs distribution in PEG/albumin particles loaded with the drug group **E**. Percentile of the distribution of albumin/PEG carriers covered with the drugs. **E'**. Insert: Percentile of NPs distribution in albumin/PEG carriers covered with the drug group.

The number of measurements for every group was equal to 6. A. Albumin particles. B. PEG/albumin particles. C. PEG/albumin particles loaded with the drugs. D. Albumin/PEG carriers covered with the drugs.

The stability of the particles was assessed under thermostatic temperature conditions of 25.0 °C. The buffer for the particles was 0.1 M PBS (pH = 7.4).

3.4. Evaluation of the Shape of the Particles

After applying LAS X software, images were obtained for all four groups: Albumin NP, albumin/PEG NP, albumin/PEG/drugs-loaded particles, and PEG/drugs-covered albumin particles (Fig. 5). The size of the particles varied from 100 nm up to several microns. The results reflect a more accurate representation of the size distribution presented above. The highest distribution of large particles was noted in the PEG/drugs-covered albumin particles group (Fig. 5A-D).

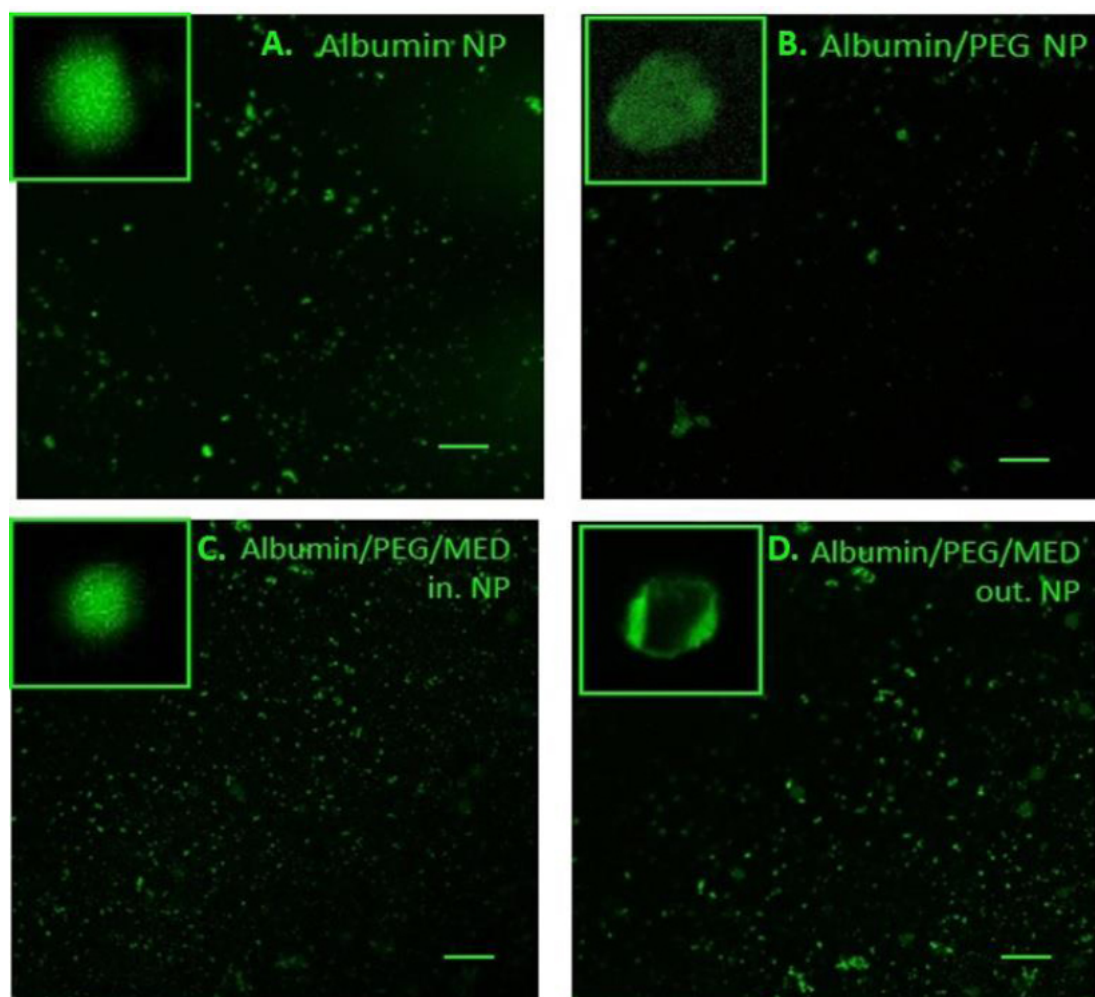


Fig. (5). Representation of the NP shapes for the different formulations of the carriers and drugs. A. Albumin NP; B. Albumin/PEG NP, C. Albumin/PEG/drugs loaded particles, D. PEG/drugs covered albumin particles. It was used with a 10x objective. The line length is 10 microns.

3.5. Degradation of Albumin, PEG/Albumin, and PEG/Albumin Particles Carrying the Drugs at 36.6 °C

3.5.1. Quantitative Evaluation of the Extent of the Degradation of the Particles based on the Measurement of the free Phase of the Drugs in the Suspension

Fig. (6) represents the degradation dynamics of the PEG/albumin particles, serving as carriers of the drugs, based on the appearance and detachment of the free drugs in the solution. The peak change in eluent consistency mostly occurred at 1.42 ± 0.099 minutes. The retention time of allopurinol in the suspension was 1.76 ± 0.085 minutes, whereas dexamethasone's was 3.32 ± 0.19 minutes. It was also found that after 15 days, a new peak appeared on the chromatograms. This peak corresponded to the degradation product of dexamethasone with a retention time of 9.44 ± 0.45 minutes.

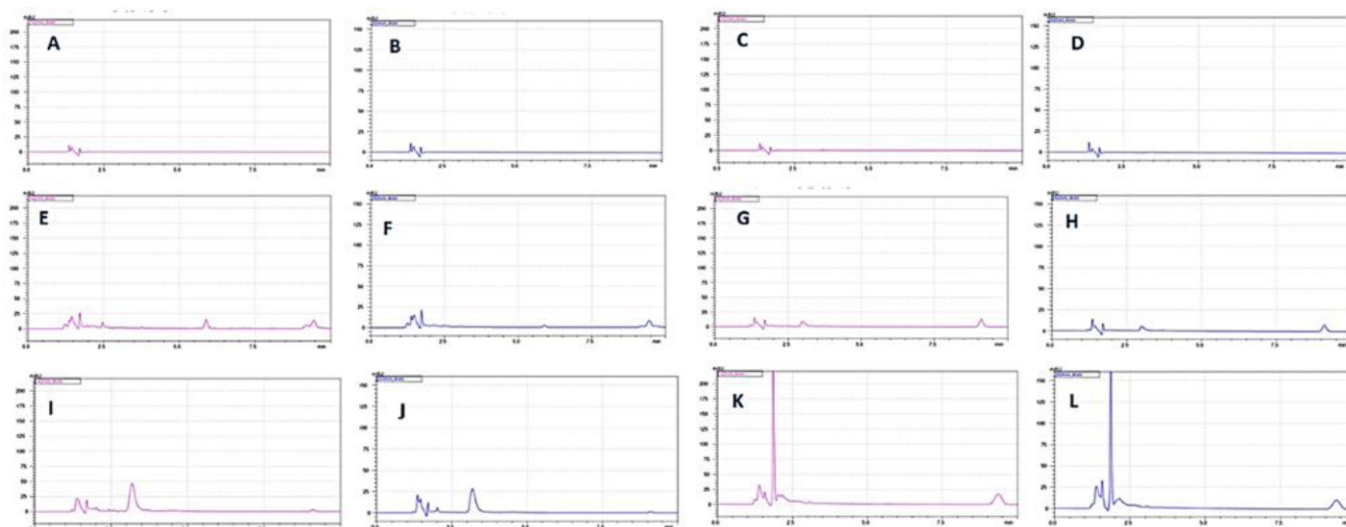


Fig. (6). Degradation at 36.6 °C of PEG/albumin particles carrying the drugs. For each group, we had $n = 5$ samples. The representative chromatograms are included in the work. Detection was carried out for allopurinol at the wavelength of 260 nm and for dexamethasone at the wavelength of 242 nm. **A.** Detection of dexamethasone, a degradation product released from PEG/albumin-coated drug particles, after 24 hours of incubation. **B.** Detection of the degradation product allopurinol from PEG/albumin particles loaded with drugs, after 24 hours of incubation. **C.** Detection of dexamethasone, a degradation product of PEG/albumin-entrapped drug particles, after 24 hours of incubation. **D.** Detection of allopurinol, a degradation product of PEG/albumin-entrapped drug particles, after 24 hours of incubation. **E.** Detection of dexamethasone, a degradation product of PEG/albumin particles coated with drugs, after 15 days of incubation. **F.** Detection of allopurinol, a degradation product of PEG/albumin particles coated with drugs, after 15 days of incubation. **G.** Detection of dexamethasone, a degradation product of PEG/albumin-entrapped drug particles, after 15 days of incubation. **H.** Detection of allopurinol, a degradation product of PEG/albumin-entrapped drug particles, after 15 days of incubation. **I.** Detection of dexamethasone, a degradation product of PEG/albumin particles coated with drugs, after 30 days of incubation. **J.** Detection of allopurinol, a degradation product of PEG/albumin particles coated with drugs, after 30 days of incubation. **K.** Detection of dexamethasone, a degradation product of PEG/albumin-entrapped drug particles, after 30 days of incubation. **L.** Detection of allopurinol, a degradation product of PEG/albumin-entrapped drug particles, after 30 days of incubation.

Based on the analysis of the results regarding the dynamic degradation of the carriers over 1 month, it was found that carriers loaded with dexamethasone and allopurinol were more stable compared to the formulations loaded with the medicines. The quantitative evaluation of the degradation extent of the particles was based on the detection of the free phase of the medicine in the suspension.

Fig. (7) represents the dynamic changes in the degradation process of the particles after one month. Fig. (6D) presents a summary of the calculated absolute amount of free, degraded protein in the suspension after one month. Fig. (6I and 6J) are graphs representing the dynamic changes in the degradation process for all groups during 24 and 48 hours of incubation at 36.6 °C.

Short-term incubation results (24 and 48 hours) demonstrated a clear difference between the stability of PEG/albumin particles compared to albumin formulations. Interestingly, as with previous experimental analyses, the PEG/albumin carriers coated with medicines during the first 24 and 48 hours were more stable than the PEG/albumin particles loaded with medicines, and this was supported by

the results from one-month incubation of the different formulation groups.

3.5.2. In vivo Circulation of the Medication Carriers

Fig. (8) represents the circulation kinetics of four formulations. PEG-coated particles persisted longer in the bloodstream compared to non-coated particles. In contrast to albumin particles, PEG-coated particles were preserved in the bloodstream, with $85.34 \pm 3.02\%$ and $83.97 \pm 3.27\%$ of the initial dosage remaining on days 3 and 7, respectively.

In comparison, PEG/albumin particles demonstrated $83.97 \pm 3.27\%$ and $42.0 \pm 3.02\%$ of the initial dosage remaining on days 3 and 7, respectively ($p < 0.05$). Albumin particles circulated for a shorter period, with only $20 \pm 2.51\%$ of the injected dosage remaining on day 3 and complete elimination by day 7 ($p < 0.02$). Interestingly, PEG/medicine-coated albumin particles were more stable in the bloodstream than particles with medicines entrapped in PEG/albumin, with $93 \pm 6.25\%$ remaining on day 3 and $75 \pm 8.25\%$ on day 7 ($p < 0.05$ compared to the initial dosage). Entrapped particles showed $85 \pm 4.15\%$ remaining on day 3 and $63 \pm 3.38\%$ on day 7 ($p < 0.035$).

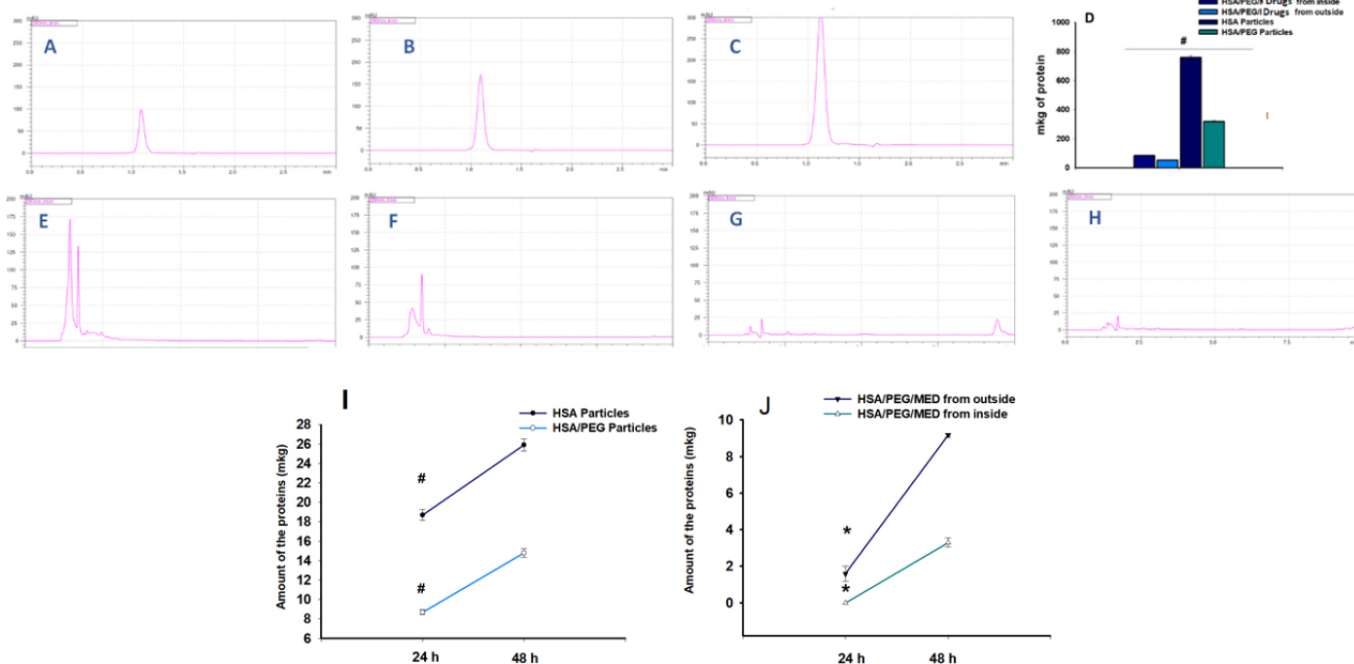


Fig. (7). The degradation of the carriers based on the quantification of the amount of the released protein at 36.6 °C during one month. For each group, we had $n = 5$ samples. The representative chromatograms are included in the work. **A., B., C.** Graph showing the linear correlation between albumin concentration and peak surface area. **D.** Calculation of the amount of the free degraded albumin in the suspension of the particles made from albumin, PEG/albumin, either coated with or containing drugs, after 1 month. **E.** Detection of degraded albumin in the suspension of albumin particles after one month, measured at 280 nm. **F.** Detection of degraded albumin in the suspension of PEG/albumin particles after one month, measured at 280 nm. **G.** Detection of degraded albumin in the suspension of PEG/albumin particles containing drugs after one month, measured at 280 nm. **H.** Detection of degraded albumin in the suspension of PEG/albumin particles coated with drug particles after one month, measured at 280 nm. **I.** Dynamic degradation process of the albumin as well as PEG/albumin particles during 24 and 48 hours (t-test, $p < 0.03$ between the groups at 24 and 48 hours' time points). **J.** Dynamic degradation process of the PEG/albumin entrapped medicines and PEG/albumin particles coated with medicine particles during 24 and 48 hours of incubation (t-test, $p < 0.05$ for 24 hours and $p < 0.03$ for 48 hours).

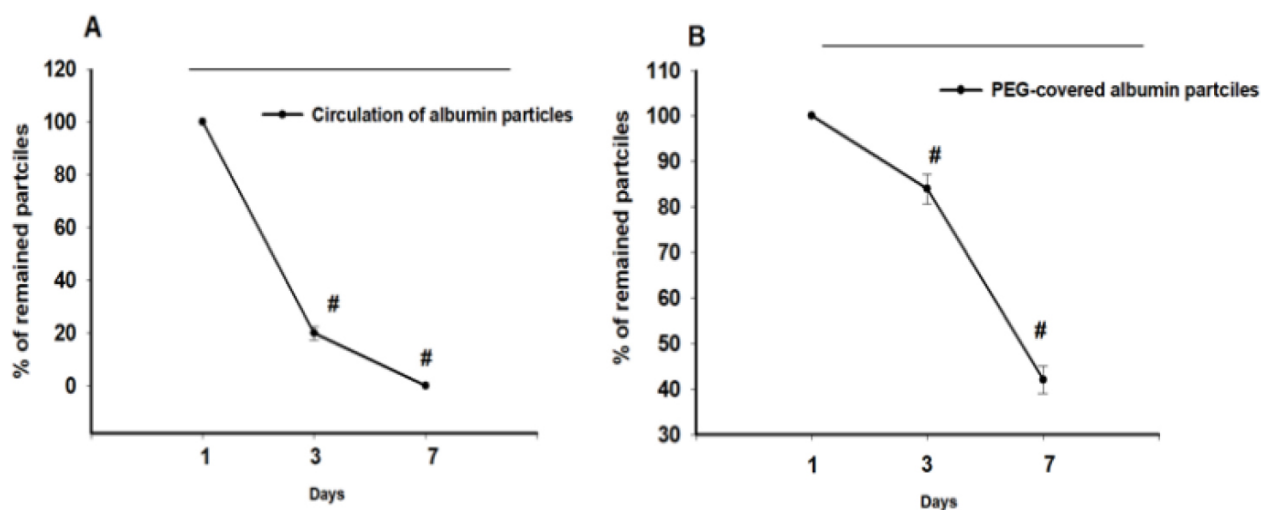


Fig. 8 contd.....

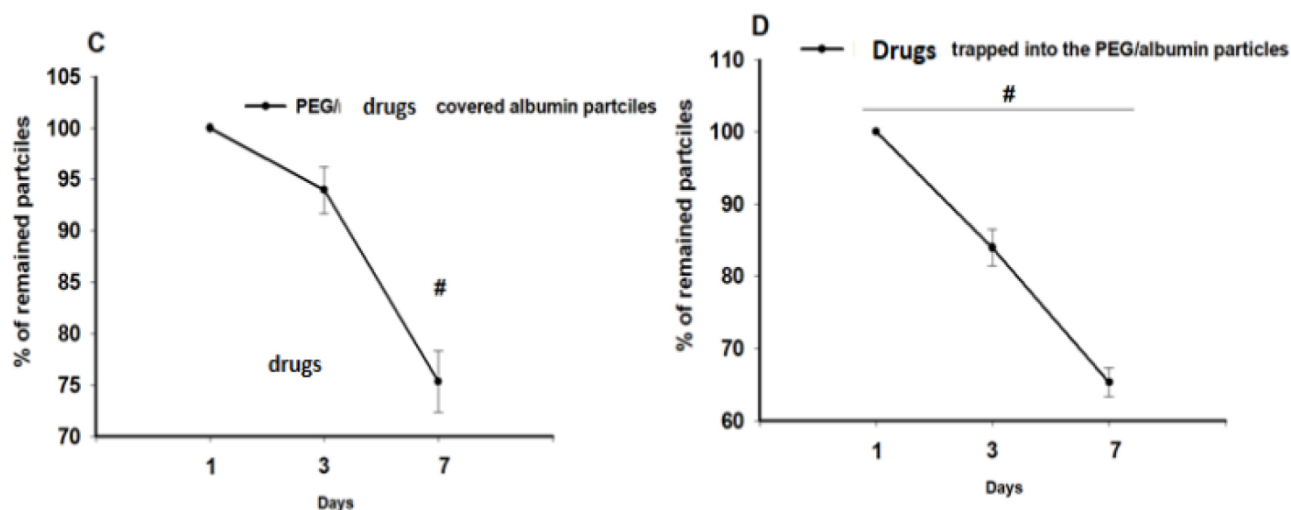


Fig. (8). Circulation of PEG-coated and uncoated albumin particles in the bloodstream of rats. N=3-5 for every group. **A.** Circulation of the albumin particles. $p < 0.002$ between days 3 and 1; $p < 0.001$ between days 1 and 7. **B.** Albumin particles, coated with PEG. $p < 0.05$ between days 1 and 7, as well as 1 and 3. **C.** Circulation of PEG/albumin particles coated with medicines ($p < 0.05$ between day 7 and the initial day). **D.** Pharmacokinetics of the PEG/albumin particles loaded with the medicines ($p < 0.05$, One-way ANOVA).

Table 2. Pharmacokinetic parameters of the carriers and the particles coated/loaded with the medicines.

Parameters	Albumin Particles	PEG-albumin Formulations	PEG/albumin Particles Coated with the Medicines	Medicines trapped in the PEG/albumin Particles
Slope	-0.04	-0.00276	-0.00095	-0.00164
k elimination	0.1	0.00635	0.00219	0.00377
T 1/2	7.2	109.14	316.73	183.7

Additionally, the elimination percentage of the particles over time was approximated as a linear dependence, allowing calculation of the half-life ($t_{1/2}$) of circulation for each group. The half-life for albumin particles was 7.2 hours, for PEG/albumin formulations, it was 4.6 days, for coated particles, it was 13.197 days, and for particles with entrapped medicines, it was 7.65 days (Table 2).

Experimental *in vivo* results provide evidence of the higher stability of PEG/albumin carriers compared to albumin particles. Formulations coated with medicines circulated in the bloodstream longer than carriers loaded with drugs.

The effects of albumin particles, PEG/albumin particles, as well as PEG/albumin particles coated with medicines and drugs entrapped into the carrier formulations, were evaluated under conditions of experimental brain oxidative injury.

We extracted Evans Blue (EB) from the ipsilateral and contralateral zones of the brain in all groups of animals: control (38.6 ± 2.0 μg ipsilateral, 29.48 ± 1.4 μg contralateral), albumin carriers (43.19 ± 3.0 μg ipsilateral, 36.46

± 1.0 μg contralateral), PEG/albumin particles (40.6 ± 1.95 μg ipsilateral, 32.35 ± 1.7 μg contralateral), PEG/albumin carriers coated with medicines (42.64 ± 1.006 μg ipsilateral, 32.7 ± 1.31 μg contralateral), and PEG/albumin particles with entrapped medicines (26.69 ± 0.025 μg ipsilateral, 23.79 ± 0.45 μg contralateral).

To account for potential variability introduced by the intracardiac perfusion procedure, we calculated the difference in Evans Blue content between the contralateral and ipsilateral hemispheres. The resulting values were as follows: for control group, it was 9.12 ± 1.2 μg ; for albumin group, it was 6.73 ± 0.58 μg ; for PEG/albumin group, it was 8.25 ± 0.52 μg ; for PEG/albumin coated with medicines, it was 9.95 ± 1.006 μg ; and for PEG/albumin with entrapped medicines, it was 2.92 ± 0.4 μg ($p < 0.04$, t-test; Fig. (9)).

The protection of the BBB was noted in two treatment groups: albumin carriers and PEG/albumin carriers loaded with medication. The effect of albumin carriers may be explained by an increase in the oncotic pressure of the blood, preventing exacerbation of BBB damage. The circulation time of albumin particles was shorter compared to PEG/albumin particles, likely due to faster degradation.

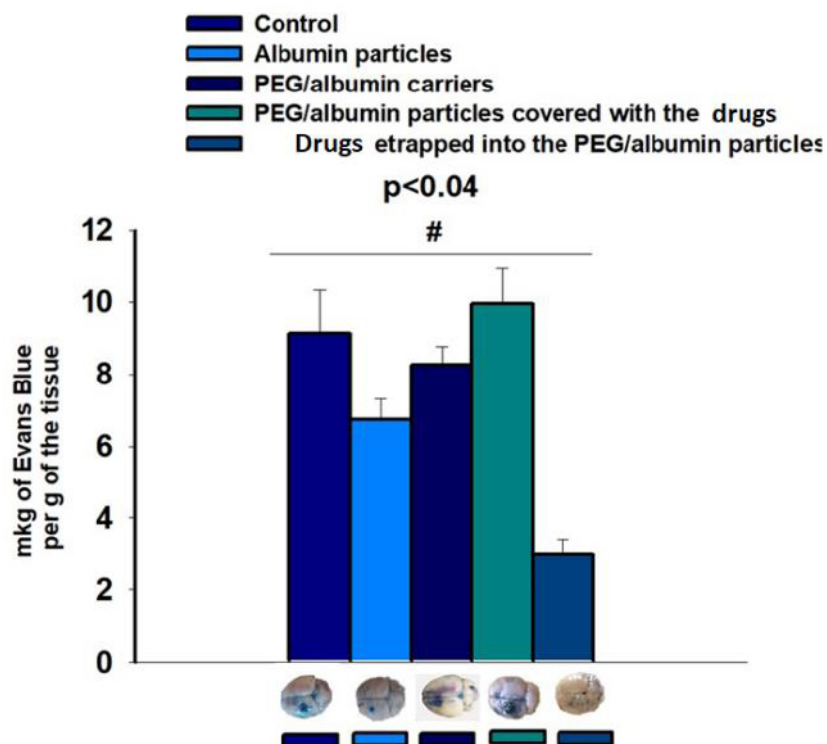


Fig. (9). The extent of blood-brain barrier (BBB) disruption in rats following the application of carriers and/or carrier-medicine formulation. N=5 for every group. A t-test was carried out. The difference between the control group and albumin particles, as well as between the control group and coated medicines, was statistically significant (\pm SD, $p < 0.04$).

Evaluation of BBB integrity was performed 7 days after brain damage, a sufficient period for degradation of albumin as well as carriers loaded with allopurinol and dexamethasone.

Numerous publications provide evidence of the neuroprotective abilities of albumin in experimental settings, including transient middle cerebral artery occlusion (MCAo) models of stroke in rats, as well as permanent occlusion of the same artery [43, 26, 44, 45]. However, clinical trials investigating the utility of albumin in humans have not been successful. Thus, animal-based experiments may not always guarantee success in clinical trials. According to published results, treatment with intravenous 25% albumin injection was not successful at 90 days and was associated with increased rates of intracerebral hemorrhage and pulmonary edema [46]. It has been observed that peptide-type compounds also possess neuroprotective abilities [47].

However, based on the results of our experiments, we propose that low dosages of albumin might be beneficial for stroke treatment, and mild elevation of oncotic pressure will not induce adverse effects, such as hemorrhage and pulmonary edema.

This study has several limitations. One limitation of this study is the formation of a small percentage of PEG/medicines or other unintended particle formulations. This is supported by observed deviations in the zeta potential measurements across the three main groups: PEG/albumin

particles, PEG/albumin particles loaded with medicines, and albumin/PEG carriers coated with medicines (Supplementary Fig. 1). Another limitation is the presence of particle populations with varying sizes. However, the primary population of particles has a diameter of about 100–200 nm.

In this study, several monomers were identified that, when combined with PEG, may be used for the development of medicine carriers, including polylysine, cholesterol, and polyinositol. We were able to develop the largest proportion of the carrier population with dominant sizes of up to 164.098 nm for the loaded formulations and 521.99 nm for those coated with drug carriers. Both formulations were highly effective in loading or coating the medicines. Based on fluorescence confocal microscopy results, the particles in all groups had round or spheroidal shapes.

After evaluating the physicochemical properties of the medicine carriers, their stability was assessed not only *in vitro* but also *in vivo*. PEG/albumin particles, as well as those coated with medicines, remained in the bloodstream longer compared to classical albumin particles and those loaded with medicine formulations. We suggest that the steroid ring of dexamethasone possesses a stabilizing effect through interaction with PEG and albumin molecules. This stabilizing effect can be explained by the formation of numerous hydrogen bonds between dexamethasone and albumin [24].

As mentioned in Table 1, cholesterol (-8.58 kcal/mol), which has a similar steroid ring, exhibited the highest binding affinity compared to other compounds.

Drug-carrying formulations remain in the bloodstream for up to 13 days, which is a sufficient period after stroke to prevent excessive immune response aggression [48], reduce the extension of brain damage, or prevent the formation of free radicals that exacerbate stroke conditions [49] due to overactivity of xanthine oxidoreductase (XOR) [50].

Considering that the main factor contributing to secondary injury following cerebral ischemia is likely brain inflammation, which accelerates neuronal death and hinders nerve tissue regeneration, the prolonged use of dexamethasone in low dosages may serve as an effective treatment regimen for stroke patients.

Finally, two formulations of nanoparticles were found to be beneficial for treating oxidative brain damage: albumin particles and carriers loaded with medicines. The first formulation possibly exerted a positive effect due to the neuroprotective nature of albumin, whereas the second showed faster degradation compared to the more stable nanoparticles loaded with medicines.

CONCLUSION

This study highlights the potential of PEG/albumin-based nanoparticles (NPs) to serve as effective carriers for drug delivery, particularly in the context of experimental stroke. Despite limitations, such as a small percentage of unintended particle formulations and broad size distributions within the particle populations, the dominant size range of 100–200 nm indicates promising uniformity in the developed spherical carriers. One area for future improvement is the application of NP surface coating techniques [51]. NPs could be coated with compounds complementary to neuronal or glial cell surface proteins expressed during brain injury [52–54].

This study has some limitations as well. One of the limitations of the study is the use of a single animal model to evaluate formulation efficacy. Hydrogen peroxide, an unstable compound that generates free radicals (FR) harmful to tissues, represents only one mechanism of brain damage and stroke development. It has been observed that no rodent model can fully replicate the complexity of clinical stroke [55]. Therefore, additional models will be employed in future studies to better clarify the overall effects of the newly developed formulations.

This study demonstrated that PEG/albumin carriers, whether loaded with or covered by drugs, exhibited pronounced stability and prolonged circulation time compared to simple albumin particles. This extended circulation may provide a promising feature of the developed particles for targeting various stages of stroke.

Hence, it can be concluded that the observed stabilizing effects, particularly with dexamethasone, are attributed to its steroid ring and hydrogen bonding potential with albumin and PEG. Cholesterol, due to its high binding affinity, also appears as a viable component for future carrier development.

Two formulations showed significant benefits: albumin-based NPs, due to their inherent neuroprotective properties, and drug-loaded carriers, due to their faster degradation and effective drug release. Thus, we successfully created stable NPs carrying different drugs, applicable for the treatment of experimental stroke. Future work should focus on optimizing particle formulations to reduce variability and further enhance clinical applicability.

AUTHORS' CONTRIBUTIONS

It is hereby acknowledged that all authors have accepted responsibility for the manuscript's content and consented to its submission. They have meticulously reviewed all results and unanimously approved the final version of the manuscript.

ETHICS APPROVAL AND CONSENT TO PARTICIPATE

This study was approved by the National Academy of Sciences of the Republic of Armenia (International Registration No. IRB0001621; IORG No. 0009782, Reference Letter (Approval N) 7, 2024).

HUMAN AND ANIMAL RIGHTS

Experiments involving animals were conducted in compliance with IACUC policies by the US National Research Council's "Guide for the Care and Use of Laboratory Animals" and animal care standards, as well as the regulations established by the Armenian Ethical Committee of the Institute of Biochemistry.

This study adhered to internationally accepted standards for animal research, following the 3Rs principle. The ARRIVE guidelines were employed for reporting experiments involving live animals, promoting ethical research practices.

CONSENT FOR PUBLICATION

Not applicable.

AVAILABILITY OF DATA AND MATERIALS

The data and supportive information are available within the article.

FUNDING

The research was supported by the Higher Education and Science Committee of MESCS RA (Research project indicative no. 21T-1F174)(funding was provided for the development of PEG/albumin and different formulations of drugs). It was also supported by a research grant from the Yervant Terzian Armenian National Science and Education Fund (ANSEF, 24AN: NS-biochem-3150, awarded to the principal investigator, K. Danielyan) based in New York, USA.

CONFLICT OF INTEREST

The authors declare no conflict of interest, financial or otherwise.

ACKNOWLEDGEMENTS

The authors would like to thank Arsen Sargsyan (PhD student) for guiding and helping with the *in situ* work organization. They would also like to thank the L.A. Orbeli Institute of Physiology, NAS RA, for providing the technical support related to fluorescence microscopy.

SUPPLEMENTARY MATERIALS

Supplementary material is available on the Publisher's website.

REFERENCES

- [1] Liu Z, Ran Y, Huang S, *et al.* Curcumin protects against ischemic stroke by titrating microglia/macrophage polarization. *Front Aging Neurosci* 2017; 9: 233. <http://dx.doi.org/10.3389/fnagi.2017.00233> PMID: 28785217
- [2] Benjamin EJ, Virani SS, Callaway CW, *et al.* Heart disease and stroke statistics - 2018 update: A report from the American Heart Association. *Circulation* 2018; 137(12): e67-e492. <http://dx.doi.org/10.1161/CIR.0000000000000558> PMID: 29386200
- [3] Alkaff SA, Radhakrishnan K, Nedumaran AM, Liao P, Czarny B. Nanocarriers for stroke therapy: Advances and obstacles in translating animal studies. *Int J Nanomedicine* 2020; 15: 445-64. <http://dx.doi.org/10.2147/IJN.S231853> PMID: 32021190
- [4] Reis C, Akyol O, Ho WM, *et al.* Phase I and Phase II therapies for acute ischemic stroke: An update on currently studied drugs in clinical research. *BioMed Res Int* 2017; 2017: 1-14. <http://dx.doi.org/10.1155/2017/4863079> PMID: 28286764
- [5] Shcharbina N, Shcharbin D, Bryszewska M. Nanomaterials in stroke treatment: Perspectives. *Stroke* 2013; 44(8): 2351-5. <http://dx.doi.org/10.1161/STROKEAHA.113.001298> PMID: 23715957
- [6] Han X, Qin Y, Mei C, Jiao F, Khademolqorani S, Nooshin Banitaba S. Current trends and future perspectives of stroke management through integrating health care team and nanodrug delivery strategy. *Front Cell Neurosci* 2023; 17: 1266660. <http://dx.doi.org/10.3389/fncel.2023.1266660> PMID: 38034591
- [7] Mitchell MJ, Billingsley MM, Haley RM, Wechsler ME, Peppas NA, Langer R. Engineering precision nanoparticles for drug delivery. *Nat Rev Drug Discov* 2021; 20(2): 101-24. <http://dx.doi.org/10.1038/s41573-020-0090-8> PMID: 33277608
- [8] Agrahari V, Burnouf PA, Burnouf T, Agrahari V. Nanof ormulation properties, characterization, and behavior in complex biological matrices: Challenges and opportunities for brain-targeted drug delivery applications and enhanced translational potential. *Adv Drug Deliv Rev* 2019; 148: 146-80. <http://dx.doi.org/10.1016/j.addr.2019.02.008> PMID: 30797956
- [9] Newland B, Taplan C, Pette D, *et al.* Soft and flexible poly(ethylene glycol) nanotubes for local drug delivery. *Nanoscale* 2018; 10(18): 8413-21. <http://dx.doi.org/10.1039/C8NR00603B> PMID: 29714385
- [10] Juneja R, Lyles Z, Vadarevu H, Afonin KA, Vivero-Escoto JL. Multimodal polysilsesquioxane nanoparticles for combinatorial therapy and gene delivery in triple-negative breast cancer. *ACS Appl Mater Interfaces* 2019; 11(13): 12308-20. <http://dx.doi.org/10.1021/acsami.9b00704> PMID: 30844224
- [11] Rackley L, Stewart JM, Salotti J, *et al.* RNA fibers as optimized nanoscaffolds for siRNA coordination and reduced immunological recognition. *Adv Funct Mater* 2018; 28(48): 1805959. <http://dx.doi.org/10.1002/adfm.201805959> PMID: 31258458
- [12] Shi D, Beasock D, Fessler A, *et al.* To PEGylate or not to PEGylate: Immunological properties of nanomedicine's most popular component, polyethylene glycol and its alternatives. *Adv Drug Deliv Rev* 2022; 180: 114079. <http://dx.doi.org/10.1016/j.addr.2021.114079> PMID: 34902516
- [13] Caballero ML, Quirce S. Excipients as potential agents of anaphylaxis in vaccines: Analyzing the formulations of currently authorized covid-19 vaccines. *J Invest Allergol Clin Immunol* 2021; 31(1): 92-3. <http://dx.doi.org/10.18176/jiaci.0667> PMID: 33433387
- [14] Mukherjee A, Sarkar S, Jana S, Swarnakar S, Das N. Neuro-protective role of nanocapsulated curcumin against cerebral ischemia-reperfusion induced oxidative injury. *Brain Res* 2019; 1704: 164-73. <http://dx.doi.org/10.1016/j.brainres.2018.10.016> PMID: 30326199
- [15] Song W, Bai L, Yang Y, *et al.* Long-circulation and brain targeted isoliquiritigenin micelle nanoparticles: Formation, characterization, tissue distribution, pharmacokinetics and effects for ischemic stroke. *Int J Nanomedicine* 2022; 17: 3655-70. <http://dx.doi.org/10.2147/IJN.S368528> PMID: 35999993
- [16] Thomas RG, Kim J, Kim J, Yoon J, Choi KH, Jeong YY. Treatment of ischemic stroke by atorvastatin-loaded pegylated liposome. *Transl Stroke Res* 2024; 15(2): 388-98. <http://dx.doi.org/10.1007/s12975-023-01125-9> PMID: 36639607
- [17] Adamczyk B, Simon J, Kitunen V, Adamczyk S, Smolander A. Tannins and their complex interaction with different organic nitrogen compounds and enzymes: Old paradigms versus recent advances. *ChemistryOpen* 2017; 6(5): 610-4. <http://dx.doi.org/10.1002/open.201700113> PMID: 29046854
- [18] Girigoswami K, Arunkumar R, Girigoswami A. Management of hypertension addressing hyperuricaemia: Introduction of nano-based approaches. *Ann Med* 2024; 56(1): 2352022. <http://dx.doi.org/10.1080/07853890.2024.2352022> PMID: 38753584
- [19] Berman H, Henrick K, Nakamura H. Announcing the worldwide Protein Data Bank. *Nat Struct Biol* 2003; 10(12): 980. <http://dx.doi.org/10.1038/nsb1203-980>
- [20] Kim S, Thiessen PA, Bolton EE, *et al.* PubChem substance and compound databases. *Nucleic Acids Res* 2016; 44(D1): D1202-13. <http://dx.doi.org/10.1093/nar/gkv951> PMID: 26400175
- [21] O'Boyle NM, Banck M, James CA, Morley C, Vandermeersch T, Hutchison GR. Open babel: An open chemical toolbox. *J Cheminformatics* 2011; 1-14.
- [22] Khallouf R, Zakaryan N, Ohanyan A, Chailyan S, Danielyan K, Hovsepyan V. Newly synthesized HV-12 prevents aggregation of the platelets via P2Y12. *Free Radic Biol Med* 2024; 224 (Suppl.): S58. <http://dx.doi.org/10.1016/j.freeradbiomed.2024.10.126>
- [23] Huey R, Morris GM, Forli S. Using AutoDock 4 and AutoDock vina with AutoDockTools: A tutorial. *Scripps Res Institute Mol Graph Lab* 2012.
- [24] Ohanyan N, Abelyan N, Manukyan A, *et al.* Tannin-albumin particles as stable carriers of medicines. *Nanomedicine* 2024; 19(8): 689-708. <http://dx.doi.org/10.2217/nnm-2023-0275> PMID: 38348681
- [25] Aganyants HA, Nikohosyan G, Danielyan KE. Albumin microparticles as the carriers for allopurinol and applicable for the treatment of ischemic stroke. *Int Nano Lett* 2016; 6(1): 35-40. <http://dx.doi.org/10.1007/s40089-015-0169-0>
- [26] Belayev L, Saul I, Busto R, *et al.* Albumin treatment reduces neurological deficit and protects blood-brain barrier integrity after acute intracortical hematoma in the rat. *Stroke* 2005; 36(2): 326-31. <http://dx.doi.org/10.1161/01.STR.0000152949.31366.3d> PMID: 15637329
- [27] Danielyan K, Ding BS, Gottstein C, Cines DB, Muzykantov VR. Delivery of anti-platelet-endothelial cell adhesion molecule single-chain variable fragment-urokinase fusion protein to the cerebral vasculature lyses arterial clots and attenuates postischemic brain edema. *J Pharmacol Exp Ther* 2007; 321(3): 947-52. <http://dx.doi.org/10.1124/jpet.107.120535> PMID: 17389242
- [28] Danielyan KE, Simonyan AA. Protective abilities of pyridoxine in experimental oxidative stress settings *in vivo* and *in vitro*. *Biomed Pharmacol* 2017; 86: 537-40. <http://dx.doi.org/10.1016/j.biopha.2016.12.053>

- [29] Gehring R. Practical pharmacokinetics for the food animal practitioner. Food Animal Practice. Research Gate 2009; pp. 460-7.
<http://dx.doi.org/10.1016/B978-141603591-6.10095-8>
- [30] Shargel L. Applied Biopharmaceutics & Pharmacokinetics. McGraw-Hill Education 2016.
- [31] Perez AS, Morikawa AT, Maranhão RC, Figueiredo Neto AM. Structural characterization of cholesterol-rich nanoemulsion (LDE). Chem Phys Lipids 2024; 263: 105418.
<http://dx.doi.org/10.1016/j.chemphyslip.2024.105418> PMID: 38944410
- [32] Hamadani CM, Mahdi F, Merrell A, *et al.* Ionic liquid coating-driven nanoparticle delivery to the brain: Applications for NeuroHIV. Adv Sci 2024; 11(23): 2305484.
<http://dx.doi.org/10.1002/adv.202305484> PMID: 38572510
- [33] Ilosvai ÁM, Gerzsenyi TB, Sikora E, *et al.* Simplified synthesis of the amine-functionalized magnesium ferrite magnetic nanoparticles and their application in DNA purification method. Int J Mol Sci 2023; 24(18): 14190.
<http://dx.doi.org/10.3390/ijms241814190> PMID: 37762494
- [34] Mo S, Li Y, Shan S, Jia L, Chen Y. Synthesis and properties of inositol nanocapsules. Materials 2021; 14(19): 5481.
<http://dx.doi.org/10.3390/ma14195481> PMID: 34639879
- [35] Nath PC, Nandi NB, Tiwari A, Das J, Roy B. Applications of nanotechnology in food sensing and food packaging. Nanotechnology Applications for Food Safety and Quality Monitoring. Academic Press 2023; pp. 321-40.
<http://dx.doi.org/10.1016/B978-0-323-85791-8.00006-9>
- [36] Opsomer L, Jana S, Mertens I, Cui X, Hoogenboom R, Sanders NN. Efficient *in vitro* and *in vivo* transfection of self-amplifying mRNA with linear poly(propylenimine) and poly(ethylenimine-propylenimine) random copolymers as non-viral carriers. J Mater Chem B Mater Biol Med 2024; 12(16): 3927-46.
<http://dx.doi.org/10.1039/D3TB03003B> PMID: 38563779
- [37] Madbouly N, Ooda A, Nabil A, *et al.* The renoprotective activity of amikacin-gamma-amino butyric acid-chitosan nanoparticles: A comparative study. Inflammopharmacology 2024; 32(4): 2629-45.
<http://dx.doi.org/10.1007/s10787-024-01464-5> PMID: 38662181
- [38] Shashni B, Nagasaki Y. Self-assembling butyric acid prodrug acts as a sensitizer for cancer radiotherapy. Nano Today 2024; 54: 102103.
<http://dx.doi.org/10.1016/j.nantod.2023.102103>
- [39] Lee BK, Yun Y, Park K. PLA micro- and nano-particles. Adv Drug Deliv Rev 2016; 107: 176-91.
<http://dx.doi.org/10.1016/j.addr.2016.05.020> PMID: 27262925
- [40] Chang X, Bao J, Shan G, Bao Y, Pan P. Crystallization-driven formation of diversified assemblies for supramolecular poly(lactic acid)s in solution. Crystal Growth & Design 2017; 17(5): 2498-506.
<http://dx.doi.org/10.1021/acs.cgd.7b00013>
- [41] Yu B, Lang X, Wang X. Effects of different conformations of polylysine on the anti-tumor efficacy of methotrexate nanoparticles. Biomed Pharmacol 2023; 162: 114662.
<http://dx.doi.org/10.1016/j.biopha.2023.114662>
- [42] Etheridge ML, Campbell SA, Erdman AG, Haynes CL, Wolf SM, McCullough J. The big picture on nanomedicine: The state of investigational and approved nanomedicine products. Nanomedicine 2013; 9(1): 1-14.
<http://dx.doi.org/10.1016/j.nano.2012.05.013> PMID: 22684017
- [43] Liu Y, Belayev L, Zhao W, Busto R, Belayev A, Ginsberg MD. Neuroprotective effect of treatment with human albumin in permanent focal cerebral ischemia: Histopathology and cortical perfusion studies. Eur J Pharmacol 2001; 428(2): 193-201.
[http://dx.doi.org/10.1016/S0014-2999\(01\)01255-9](http://dx.doi.org/10.1016/S0014-2999(01)01255-9) PMID: 11675036
- [44] Rodriguez de Turco EB, Belayev L, Liu Y, *et al.* Systemic fatty acid responses to transient focal cerebral ischemia: Influence of neuroprotectant therapy with human albumin. J Neurochem 2002; 83(3): 515-24.
<http://dx.doi.org/10.1046/j.1471-4159.2002.01121.x> PMID: 12390513
- [45] Belayev L, Pinard E, Nallet H, *et al.* Albumin therapy of transient focal cerebral ischemia: *In vivo* analysis of dynamic microvascular responses. Stroke 2002; 33(4): 1077-84.
<http://dx.doi.org/10.1161/hs0402.105555> PMID: 11935064
- [46] Martin RH, Yeatts SD, Hill MD, Moy CS, Ginsberg MD, Palesch YY. ALIAS (albumin in acute ischemic stroke) trials. Stroke 2016; 47(9): 2355-9.
<http://dx.doi.org/10.1161/STROKEAHA.116.012825> PMID: 27462118
- [47] Galoyan AA, Kriegelstein J, Klumpp S, *et al.* Effect of hypothalamic proline-rich peptide (PRP-1) on neuronal and bone marrow cell apoptosis. Neurochem Res 2007; 32(11): 1898-905.
<http://dx.doi.org/10.1007/s11064-007-9379-9> PMID: 17549627
- [48] Zheng Y, Ren Z, Liu Y, *et al.* T cell interactions with microglia in immune-inflammatory processes of ischemic stroke. Neural Regen Res 2025; 20(5): 1277-92.
<http://dx.doi.org/10.4103/NRR.NRR-D-23-01385> PMID: 39075894
- [49] Hou Z, Brenner JS. Developing targeted antioxidant nanomedicines for ischemic penumbra: Novel strategies in treating brain ischemia-reperfusion injury. Redox Biol 2024; 73: 103185.
<http://dx.doi.org/10.1016/j.redox.2024.103185> PMID: 38759419
- [50] Chen X, Zeng Q, Tao L, *et al.* Machine learning-based clinical prediction models for acute ischemic stroke based on serum xanthine oxidase levels. World Neurosurg 2024; 184: e695-707.
<http://dx.doi.org/10.1016/j.wneu.2024.02.014> PMID: 38340801
- [51] Morshedi B, Esfandyari-Manesh M, Atyabi F, Ghahremani MH, Dinarvand R. Local delivery of ibuprofen by folate receptor-mediated targeting PLGA-PEG nanoparticles to glioblastoma multiform: *In vitro* and *in vivo* studies. J Drug Target 2025; 33(6): 1026-41.
<http://dx.doi.org/10.1080/1061186X.2025.2468749> PMID: 39960788
- [52] Johns AE, Taga A, Charalampopoulou A, *et al.* Exploring P2X7 receptor antagonism as a therapeutic target for neuroprotection in an hiPSC motor neuron model. Stem Cells Transl Med 2024; 13(12): 1198-212.
<http://dx.doi.org/10.1093/stcltm/szae074> PMID: 39419765
- [53] Howard EM, Strittmatter SM. Development of neural repair therapy for chronic spinal cord trauma: Soluble Nogo receptor decoy from discovery to clinical trial. Curr Opin Neurol 2023; 36(6): 516-22.
<http://dx.doi.org/10.1097/WCO.0000000000001205> PMID: 37865850
- [54] Cai XF, Lin S, Geng Z, *et al.* Integrin CD11b deficiency aggravates retinal microglial activation and RGCs degeneration after acute optic nerve injury. Neurochem Res 2020; 45(5): 1072-85.
<http://dx.doi.org/10.1007/s11064-020-02984-6> PMID: 32052258
- [55] Ginsberg MD, Busto R. Rodent models of cerebral ischemia. Stroke 1989; 20(12): 1627-42.
<http://dx.doi.org/10.1161/01.STR.20.12.1627> PMID: 2688195

DISCLAIMER: The above article has been published, as is, ahead-of-print, to provide early visibility but is not the final version. Major publication processes like copyediting, proofing, typesetting and further review are still to be done and may lead to changes in the final published version, if it is eventually published. All legal disclaimers that apply to the final published article also apply to this ahead-of-print version.